

Total Measurement Uncertainty Estimation For Tomographic Gamma Scanner

R.Venkataraman¹, S.Croft¹, M.Villani¹, R.D. McElroy¹, and R.J. Estep²

¹Canberra Industries, Inc., 800 Research Parkway, Meriden, Connecticut, 06450, USA.

²Advanced Nuclear Technology Group (N-2), Los Alamos National Laboratory,
Los Alamos, New Mexico 87545, USA.

Abstract

Radioactive waste contained in drums can be highly heterogeneous in matrix distribution and may also exhibit a non-uniform and unrelated distribution of radionuclides. Under such circumstances, accurate quantitative results can be obtained by performing non-destructive assay of the waste using a Tomographic Gamma Scanner (TGS). The TGS combines high-resolution gamma spectrometry and low spatial resolution 3-dimensional transmission and emission imaging techniques to accomplish assay goals. The transmission image is a voxel-by-voxel distribution of linear attenuation coefficients throughout the drum volume, and the emission image is a voxel-by-voxel distribution of the source activity. The TGS technique is well suited for low to moderate density waste matrices, say 1.0 g.cm^{-3} or below for 55 U.S. gal. drums, although it can be extended to higher densities by using alternative approaches to the analyses. These include the uniform layer and the bulk density analyses. In the uniform layer approach, all the voxels in a given drum layer (or segment) are populated with the same average value of linear attenuation coefficient. In the bulk density approach all of the voxels in all the drum layers are populated with the same value of linear attenuation coefficient.

The TGS technique can tolerate a higher degree of matrix heterogeneity and a greater non-uniformity of the source distribution than other, non-imaging, γ -ray techniques. However, the method is not immune to radial biases and source distribution dependent errors. For source positions that are at the boundary between two layers, the assay results may be biased depending on the location of the emission image. In general, these biases tend to get worse with increasing matrix densities. An extensive measurement campaign was undertaken by Canberra Industries to study the above mentioned biases and quantify the Total Measurement Uncertainty (TMU) for the TGS technique. Point sources of ^{137}Cs and ^{60}Co were located inside drum matrices whose densities ranged from 0 g.cm^{-3} to 2.9 g.cm^{-3} and assayed using the TGS. To study the radial bias, single point sources of ^{137}Cs and ^{60}Co were co-located at different radial positions and assayed. To study the source distribution dependent error, three point sources of ^{137}Cs and three of ^{60}Co were distributed randomly inside a given drum matrix and assayed using the TGS. This is based on the postulate that a typical waste drum is likely to contain at least 3 equivalent point sources randomly distributed in the drum volume rather than a single localized source. For each matrix drum, fifteen such random source distributions were generated and assayed. This was repeated for six matrix drums with densities ranging from 0 g.cm^{-3} to 2.9 g.cm^{-3} . To study the effect of an emission source at a layer boundary, a point source of ^{137}Cs and ^{60}Co were co-located inside a drum matrix at a given radial position and at the boundary between 2 segments and assayed. The measurements were repeated for a few radial positions and for drums with different matrix densities.

The present paper describes the challenges posed by difficult to assay waste along with the experiments and analyses used to construct the uncertainty contributions.

1. Introduction

The Tomographic Gamma Scanner (TGS) is a High Resolution Gamma Spectrometry (HRGS) based instrument that is being increasingly employed to perform non-destructive assay of radioactive waste. The TGS methodology combines low spatial resolution imaging techniques with HRGS and in certain situations can yield quantitative results that are more accurate when compared to non-imaging methods^[1-3]. In a TGS assay, the waste drum is scanned with three degrees of freedom, (i.e. rotation, translation and elevation). The waste drum is typically divided into 16 vertical segments, and at every segment two scans are performed. In the transmission scan, a highly collimated gamma ray source is used to interrogate the waste matrix. In the emission scan, the transmission source is not exposed, and the detector views the gamma ray emissions from radionuclides within the item. The TGS scan sequence generates a series of data grabs or views which over determine the contents of the voxels. Algebraic reconstruction in real space is used to extract a best fit solution consistent with the data and as free from spurious features as possible. The transmission data is used to determine the linear attenuation coefficient map (transmission image). The emission data is used to solve for the radionuclide distribution on a voxel-by-voxel basis, which is then corrected for photon attenuation using the transmission map.

As in any NDA method, the Total Measurement Uncertainty (TMU) budget must be quantified for the TGS for a proper interpretation of the assay results. In this paper, we estimate the TMU contributions due to radial biases, source non-uniformity, and errors due to source being located at the boundary between 2 segments for 208 liter drums. The TMU estimates are obtained for several drums matrices in the density range between 0.4 g.cm^{-3} to 1.0 g.cm^{-3} . The results for high densities will be presented in a future report.

2. The TGS System

The TGS system used in the measurement campaign for estimating TMU consists of a coaxial Canberra High Purity Germanium (HPGe) detector with a 120% relative efficiency and a 7 mCi ^{152}Eu transmission source. The detector is housed inside a 50mm thick cylindrical lead shield with a low-Z inner liner and is collimated. The collimating aperture is formed by interleaved layers of lead or tungsten that can be opened or closed. In the present work, the width of the diamond collimator aperture was set equal to 50.8 mm (or 2 inches). The transmission source is housed inside a shielded assembly. The source can be exposed by opening a tungsten shutter. The detector and transmission assemblies and the rotating platform were carefully aligned mechanically. The mechanical movements are controlled by a GE FANUC Programmable Logic Controller (PLC).

The pulse processing electronics consists of a Transistor Reset Pre-amplifier, a Canberra Model 2060 Digital Signal Processor (DSP), and an Accuspec B Board to facilitate high speed data transfer, and a Canberra Model 1654 NIM Reference Pulser. Rate loss corrections were performed using the reference pulser counts. Data acquisition and analysis was performed using Canberra's NDA2000 software platform.

The DSP gain was adjusted and the energy and Full Width Half Maximum (FWHM) calibrations were carried out on the detector. The Regions of Interest (ROI) were set up around the gamma ray peaks of interest as well as the left and right continuum regions around those peaks. The ROIs were set up for both transmission and emission gamma ray peaks of interest.

Figure 1 shows a picture of the fully automated TGS system that Canberra has recently built. The TGS system used in the present work uses a collimator configuration and measurement geometry similar to the fully automated TGS.



Figure 1. Canberra's fully automated TGS system

The drum handling system is between the transmission lift and the detector lift. The touch screen local PLC control is on the right. The collimator aperture, detector horizontal position and lead filters in front of the detector are automatically adjusted based on drum dose rates. The dose rate is measured by a dosimeter mounted in front of the detector collimator assembly.

3. TGS Assays to Estimate TMU

The TGS assays were performed by locating point sources of ^{137}Cs and ^{60}Co inside 208 liter drums containing different matrices. The drum matrices used were Empty, Homosote (0.43 g.cm^{-3}), Particle Board (0.72 g.cm^{-3}) and Scrap Steel (bulk density of 1.0 g.cm^{-3}). Assays were also performed using higher density matrices such as Sand (1.60

g.cm⁻³), Heavy Steel (bulk density of 2.0 g.cm⁻³) and Concrete mixture including steel (bulk density of 2.9 g.cm⁻³), but the analysis on these is on-going and will be reported elsewhere.

3.1 Radial bias

The present TGS method cannot faithfully image a point source at the center of the drum. Since a 10 x 10 voxel grid is used in the reconstruction, the image at best will be distributed among the 4 central voxels. In other words, the image is pushed outward, thus resulting in a smaller attenuation correction and a low bias in the emission results. For a source at the outer edge of the drum, the solutions exist towards the interior of the drum. The image tends to get pushed inward, thus resulting in high bias. Thus a radial bias does exist in TGS results and is accentuated by poor counting statistics. To estimate the error contribution due to radial bias, a point source of ¹³⁷Cs and ⁶⁰Co were co-located at several different radial positions inside a given drum matrix and assayed. The activities of the ¹³⁷Cs and ⁶⁰Co point sources were 59.5 µCi and 56.9 µCi, respectively. Each assay was performed for the duration of 1 hour. This translates to a scanning time of 112.5 sec per segment of the drum. During each scan, 150 full spectral (8K channels) views or data grabs are acquired, each view lasting for a time period of 0.75 seconds. For all drums except the Scrap Steel drum, the sources were assayed at 9 different radial locations, starting from the center of the drum to the outer edge. The radial locations were distributed in a spiraling fashion. At each radius, the sources were located at the mid-plane of the drum. The Scrap Steel drum had a non-homogeneous matrix with chunks of metal and air gaps, and only six radial positions could be realized.

The TGS results are given in terms of the “TGS Number” at each gamma ray of interest. The TGS number is proportional to nuclide activity and has all of the corrections such as those due to attenuation and rate loss already applied to it. In other words, the TGS number per unit activity of a nuclide must be the same at a given gamma ray energy irrespective of the drum matrix.

For each drum matrix, a radially weighted average of the TGS response is determined. To quantify the bias, two ratios, R_{\min} and R_{\max} are defined where R_{\min} is the ratio of minimum TGS response with respect to the radial average and R_{\max} is the maximum TGS response with respect to the radial average. The difference ($R_{\max} - R_{\min}$) is taken as the extreme range which we approximate as $\pm 3\sigma$ (i.e. 6σ span). Further, it is postulated that a typical waste drum is likely to contain at least three equivalent point sources randomly distributed in the drum volume. The 1σ relative standard deviation can be approximated as:

$$RSD_{\text{radial}} = \frac{(R_{\max} - R_{\min})}{6\sqrt{3}} \quad (1)$$

In equation (1) the factor square root of 3 in the denominator is to accommodate the 3 point source assumption. It must be noted that the difficult case of a point source at the center of the drum was included as part of the data set. Table 1 gives the radial bias values as a function of matrix density.

Table 1. Bias due to Radial location

Drum	Density (g. cm ⁻³)	662 keV			1173 keV			1332 keV		
		R _{min}	R _{max}	RSD	R _{min}	R _{max}	RSD	R _{min}	R _{max}	RSD
Empty	0.0	0.9261	1.0338	0.0104	0.9054	1.0248	0.0115	0.9057	1.0218	0.0112
Homosote	0.43	0.9466	1.0637	0.0113	0.9704	1.0287	0.0056	0.9780	1.0218	0.0042
Part. Brd	0.72	0.9216	1.1243	0.0195	0.9359	1.0878	0.0146	0.9413	1.0734	0.0127
Scrap steel	1.0	0.9250	1.0607	0.0131	0.9434	1.0478	0.0100	0.9463	1.0253	0.0076

From Table 1, it is evident that the TMU contribution due to radial bias is in the 1%-2% range at the gamma ray energies and matrix densities investigated, when the matrix specific normalization is used.

The point source images are shown for the particle board drum as an example (Figures 2a and 2b). These correspond to emission gamma ray energies of 662 keV and 1332 keV. In these figures, the transmission (linear attenuation coefficient) images are on the left and the emission images are on the right. The bottom images are summed views (similar to radiographs), and the top images are layer slice views. The one layer shown is indicated on the side view by tic marks on either side. The images correspond to a radial location of 217 mm. The point sources are present in segment 7 of the drum.

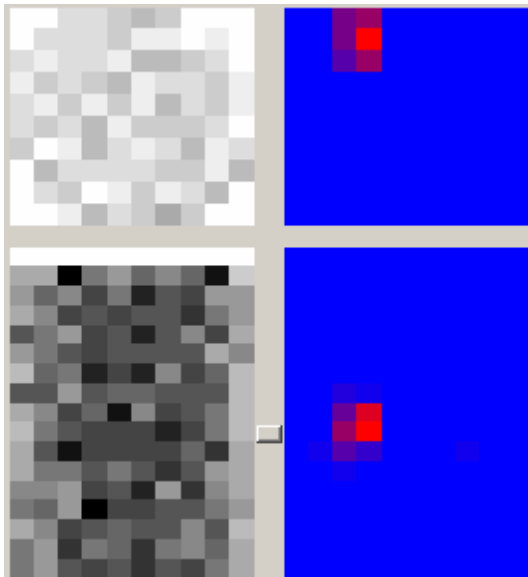


Fig.2a ¹³⁷Cs point source in Particle Board drum

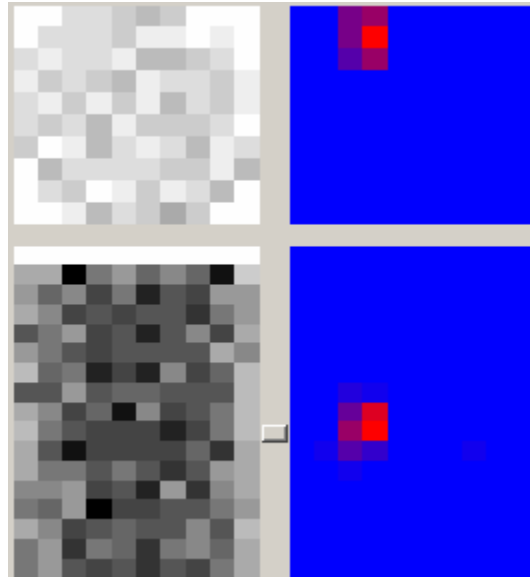


Fig.2b ⁶⁰Co point source in Particle Board drum

The accuracy of the TGS results as a function of matrix density was determined by obtaining the bias in the matrix drum results with respect to the empty drum results. The radial average of TGS Number per unit activity of a given nuclide for the matrix drum was compared against the same quantity for the empty drum. The bias estimates are given in Table 2.

Table 2a. Accuracy of TGS results as a function of matrix density

Matrix	Density (g.cm ⁻³)	662 keV		1173 keV		1332 keV	
		TGS/μCi	Bias	TGS/μCi	Bias	TGS/μCi	Bias
Empty	0.0012	0.0819	0	0.0748	0	0.0707	0
Homosote	0.43	0.0731	-10.72%	0.0705	-5.82%	0.0666	-5.81%
Part Brd	0.72	0.0695	-15.08%	0.0676	-9.60%	0.0645	-8.73%
Scrap steel	1.0	0.0693	-15.31%	0.0675	-9.83%	0.0645	-8.72%

The accuracy of TGS results are in the 10%-15% range at 662 keV and in the 5%-10% range at higher energies when one compares the radial average of the results. However, in the analysis, if a correction factor of 1.2 is applied to the attenuation coefficients at the emission energies it seems to mitigate the bias in the results, as shown in Table 2b. The capability to make this empirical allowance is present in the TGS analysis code. The source of this bias in the TGS technique is being investigated and will be reported in the near future. It must be noted that the bias in the results can be alleviated by calibrating the system with a representative matrix drum rather than the empty drum.

Table 2b. Accuracy of TGS results including the attenuation coefficient correction factor

Matrix	Density (g.cm ⁻³)	662 keV		1173 keV		1332 keV	
		TGS/μCi	Bias	TGS/μCi	Bias	TGS/μCi	Bias
Empty	0.0012	0.0833	0.00%	0.0758	0.00%	0.0716	0.00%
Homosote	0.43	0.0816	-2.05%	0.0775	2.18%	0.0730	1.97%
Part Brd	0.72	0.0799	-4.17%	0.0759	0.14%	0.0721	0.72%
Scrap steel	1.0	0.0898	7.73%	0.0840	10.75%	0.0780	9.05%

3.2 TGS performance based on Random distribution of 3 Point Sources

The overall performance of the TGS method was determined by randomly distributing three point sources of ¹³⁷Cs and ⁶⁰Co inside the drum volume and assaying the drum. TGS assays were performed for fifteen such random 3-point source distributions per matrix drum. The mean and standard deviation of the TGS results were determined for each drum. The scatter results are given in Table 4. These results include variations due to source distribution, matrix heterogeneity as well as counting statistics. Also, note that the 3 point source measurements are checks on the uncertainty estimates derived using the single point source scans. The statistical precision is estimated independently using the Monte Carlo Randomization (MCR) method^[4] for an individual assay, but is amenable to replicate assays of the same item.

Table 4. TGS Uncertainty as function of matrix density

Matrix	Density (g. cm ⁻³)	TGS Uncertainty (1σ)		
		662 keV	1173 keV	1332 keV
Empty	0.0012	4.20%	3.68%	3.65%
Homosote	0.43	6.34%	4.18%	3.87%
Particle Board	0.72	6.73%	5.68%	5.68%
Scrap Steel	1.0	14.58%	10.36%	9.99%

The transmission and emission images for one of the random 3 point source distributions are shown for the Particle Board drum since this matrix represents a median density. Figures 3a and 3b are the images at the gamma ray energies of 662 keV and 1332 keV.

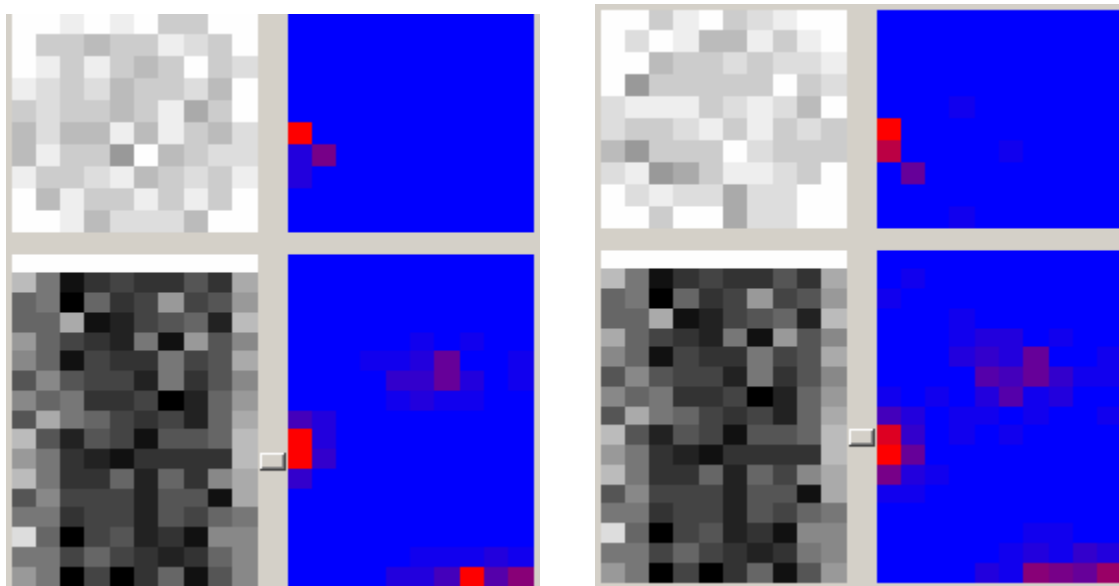


Fig.3a A 3 ¹³⁷Cs point source distribution in Part Brd Fig.3b A 3 ⁶⁰Co point source distribution in Part Brd

The overall performance for the homogeneous matrices are very reasonable. In the case of the Scrap Steel matrix, a reason for worsening of the uncertainty could be because of the matrix inhomogeneity.

3.3 Layer Boundary Effects

Another potential source of uncertainty could be because of the source being present at the boundary between two layers (or segments). In this case, since source is represented at the center of a voxel, the image reconstruction algorithm (Expectation Maximization or EM algorithm) has to divide the contribution between 2 voxels. Furthermore, layer coupling effects may also play a role. There could also be variations due to the attenuation values in the 2 voxels. To investigate this, point sources of ¹³⁷Cs and ⁶⁰Co were located at the boundary between 2 drum segments (10 and 11) and assayed. The assays were performed at a few of the same radial positions as in the measurements to

determine the radial bias. The TGS results for the layer boundary assays were compared against the corresponding “in-layer” results at the same radial location. The ratio of the layer boundary TGS results with respect to the “in-layer” results are given in Tables 5 and 6 for the Homosote and Particle Board matrices, respectively.

Table 5. Ratio of Layer Boundary TGS result with respect to “in-layer” result (Homosote matrix)

Radial position, mm	662 keV		1173 keV		1332 keV	
	Ratio	Uncertainty	Ratio	Uncertainty	Ratio	Uncertainty
0	1.000	0.052	1.024	0.043	1.031	0.036
143	0.992	0.039	0.967	0.034	0.948	0.031
217	1.032	0.062	0.974	0.038	0.994	0.036
273	0.860	0.053	0.878	0.036	0.883	0.034
Mean	0.971		0.961		0.964	

Table 6. Ratio of Layer Boundary TGS result with respect to “in-layer” result (Particle Board matrix)

Radial position, mm	662 keV		1173 keV		1332 keV	
	Ratio	Uncertainty	Ratio	Uncertainty	Ratio	Uncertainty
0	1.001	0.061	1.013	0.053	0.998	0.050
143	0.968	0.045	0.981	0.034	0.944	0.031
217	0.877	0.059	0.883	0.047	0.913	0.042
273	1.017	0.066	1.002	0.043	0.997	0.036
Mean	0.966		0.970		0.963	

The uncertainty estimates in the ratios given in Tables 5 and 6 are based on the random uncertainties calculated using the MCR method. For the Homosote matrix, the results at all radial positions except the outermost are within 1σ of the uncertainty bounds. In the case of the Particle Board matrix, the results for radial position of 217 mm are outside of the uncertainty bounds whereas all others are within 1σ . Since the anomaly does not occur at the same radial position for the two matrices, it may not be a systematic problem with imaging, but could be because of statistical fluctuations in the view data. The mean of the ratio between layer boundary to in-layer TGS results was taken and its deviation from unity is taken as a measure of uncertainty due to layer boundary effects. There does not appear to be a clear trend in the results. There are, however, some outliers which are of worthy of repeating.

The TGS images for the Homosote matrix are given in Figures 4a and 4b.

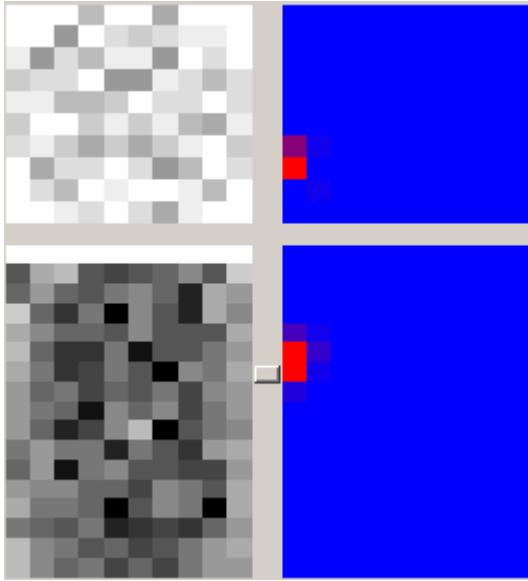


Fig.4a ^{137}Cs point source between layers 10 and 11

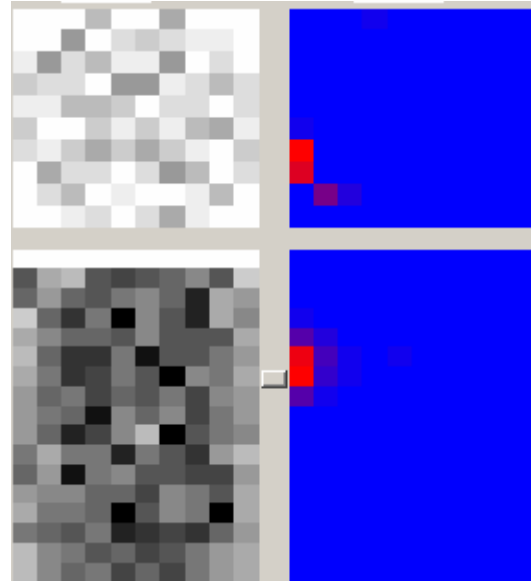


Fig.4b ^{60}Co point source at between layers 10 and 11

4. Conclusions

The contribution to the total measurement uncertainty estimate, from three different sources of errors, according to the conventional definition of TMU applied within NDA2000 software, was investigated in this work. The focus was on matrix densities up to a maximum of 1.0 g.cm^{-3} . The three sources of errors discussed in this work were: (1) the bias associated with the radial position of the source, (2) the scatter in the TGS results, based on random distributions of 3 point sources, (3) layer boundary effects. The radial bias for the matrices that were investigated were in the 1% - 2% range at the gamma ray energies that were considered. The scatter in the TGS results, based on the 3 point source distribution was in the 4%-6% range for homogeneous matrices. For the non-homogeneous Scrap steel matrix, the scatter was greater (14%) indicating the impact of matrix heterogeneity. No particular trend was discernable due to layer boundary effects, but additional measurements are being planned to verify this. Statistical uncertainties were determined for each individual assay based on the MCR method.

Higher density drums have been assayed and the analysis is ongoing. New approaches such as uniform layer analysis and bulk density analysis are being applied on these difficult cases as the statistical quality of the grab data deteriorates. The results will be reported elsewhere.

5. References

1. S. Croft, TD Anderson, R.J. Estep, R.J. Huckins, D.L. Petroka, R. Venkataraman and M. Villani, *A new drum tomographic gamma scanning system*, Presented at

- the 25th ESARDA Symposium on Safeguards and Nuclear Material Management, Stockholm, Sweden, 13-15 May 2003.
2. S. Croft, R. Venkataraman, and M. Villani, *Characterizing a Tomographic Gamma Scanner*, Proceedings of 45th Annual INMM Meeting, Orlando, FL, July 18-22, 2004.
 3. R. Venkataraman, S. Croft, M. Villani, and R.J. Estep, *Performance Study of the Tomographic Gamma Scanner for the Radioassay of drums*, Proceedings of 45th Annual INMM Meeting, Orlando, FL, July 18-22, 2004.
 4. R.J. Estep, D. Miko, and S. Melton, Monte Carlo error estimation applied to Nondestructive Assay methods, Nondestructive Assay Waste Characterization Conference, Salt Lake City, Utah, May 22-26, 2000.